Beam-Steerable Flat Reflector via Transformation Electromagnetics

R. Yang[1,2], W. X. Tang[1], and Y. Hao[1]
[1] School of Electronic Engineering and Computer Science. Queen Mary University of London, London E1 4NS, U.K
[2] School of Electronic Engineering. Xidian University, Xi'an 710071, China

***Abstract*-Instead of off-axis feeding or tilting reflector axis, we show an alternative way to manipulate the reflected emission by tuning coordinate transformation based dielectrics. Such a technique keeps the same flat profile of the reflector system without displacements between the feed and reflector, while processing the ability to steer the radiation beams.**

I. Introduction

Transformation optics as a practical strategy to control lights has been intensively studied and widely adopted recently. It opened a fresh research direction that connects the geometrical optics and the gradient refractions of electromagnetic materials, thus has initiated the quest for cloaking as well as other electromagnetic applications [1-3]. However, one of the biggest hurdles of various transformation-based designs is a lack of practical realizations since constitutive parameters produced in transformations are often very complicated and can not be found from natural materials. Potential solution proposed recently by using a discrete coordinate transformation and proper approximations has led to all dielectric transformed devices rather than those based on metamaterials, which makes this technique much more attractive in practical applications [4-9].

This paper extends the above principle to the flat reflector design [10-15]. 20×5 dielectric blocks instead of metamaterials with simultaneously dispersive permittivity and permeability are employed to the flat reflector aperture. Besides the conventional off-axis feeding or tilting reflector axis, we investigate an alternative way to manipulate the reflected emission by tuning coordinate transformation baseded dielectrics. Such a technique keeps no change of the relative position of the flat reflector and its feeding, while processing the ability to steer the radiation beams.

II. Theory and Numerical Results

A. Flat reflector

For simplicity, we only consider the two-dimensional coordinate transformation between the parabolic reflector and the flat reflector. The permittivity and permeability tensors in virtual space ($\bar{\bar{\varepsilon}}$, $\bar{\bar{\mu}}$) and physical space ($\bar{\bar{\varepsilon}}'$, $\bar{\bar{\mu}}'$) have the relation of $\bar{\bar{\varepsilon}}' = J\bar{\bar{\varepsilon}}J^T/\det(J)$ and $\bar{\bar{\mu}}' = J\bar{\bar{\mu}}J^T/\det(J)$, where J is the Jacobian transformation matrix between the local distorted and Cartesian coordinates [3]. It has been proven [4] that the effective refractive index for E-polarization incidence could be dependant only on the permittivity value as long as the grid is carefully generated into nearly orthogonal cells in the virtual space as shown in Fig. 1(a). The demonstration parabolic reflector [16] has an aperture $D = 10\lambda$ and the focal length $F = 5\lambda$. The designed working frequency is 15 GHz, with a wavelength of $\lambda = 20$ mm in free space. Fig. 1(b) illustrates the orthogonal grid of Cartesian cells with the permittivity map consisting of 92 × 16 blocks. So far, a conventional parabolic reflector in the virtual space has been completely compressed into the flat reflector in the physical space. A further step to approximate and simplify the transformation optics is based on a recent design approach used in an implementation of a simplified carpet cloak made of only a few blocks of all-dielectric isotropic materials [8]. When applied to the present work, the high resolution permittivity map shown in Fig 1(b) can thus be approximated using a relatively low resolution sampling map with 30×5 sampled block in the transformed reflector, shown in Fig. 1(c).

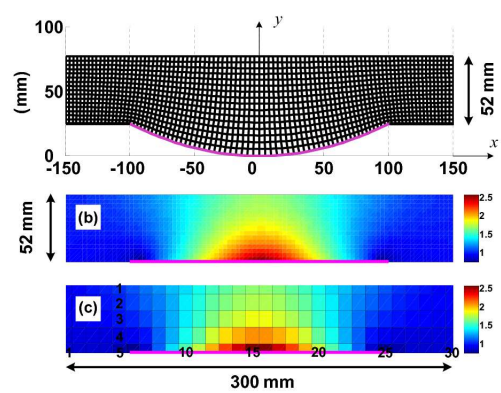

Fig. 1. Discrete Coordinate transformation for the parabolic reflector and the flat reflector design. (a) Conventional parabolic reflector set in the air with nearly orthogonal mapping. The purple line from -100 mm to 100 mm refers to the reflector made of PEC. (b) Flat reflector with the permittivity map consisting of 92×16 dielectric blocks. The curved reflector is replaced by a flat PEC sheet as shown by the purple line from -100 mm to 100 mm. (c) Flat reflector with the permittivity map consisting of 30×5 blocks. The five layers have heights of 6.5mm, 13mm, 13mm, 13mm and 6.5mm respectively in the y direction, and the 1st and 30th unit cells have the width of 5.24mm in x direction and the rest from 2nd unit cell to the 29th unit cell have a width of 10.34mm.

A full-wave finite-element simulation (Ansoft HFSS v12) is then performed to verify the proposed design. Fig. 2 shows the

normalized E field distribution on the x-y plane with z = 0 in the conventional parabolic reflector and 30 × 5-block flat reflector. On the one hand, both reflectors have almost the same focusing point at the focal point as depicted in Fig. 2(a) and Fig. 2(b). On the other hand, in Fig. 2(c) and Fig. 2(d), nearly the same plane wave is generated by both devices when we feed them on the focal points. The E field is normalized by 2.88×10^3 V/m and 3.58×10^3 V/m respectively for the parabolic reflector and the flat reflector with the same plane wave incidence, while the E field is normalized by 2.28×10^3 V/m and 2.23×10^3 V/m respectively for the parabolic reflector and the flat reflector with the same waveguide excitation at the focal point. There is slightly difference between the refraction patterns of two reflectors, which mainly originates from neglecting the anisotropy derived from the discrete coordinate transformation.

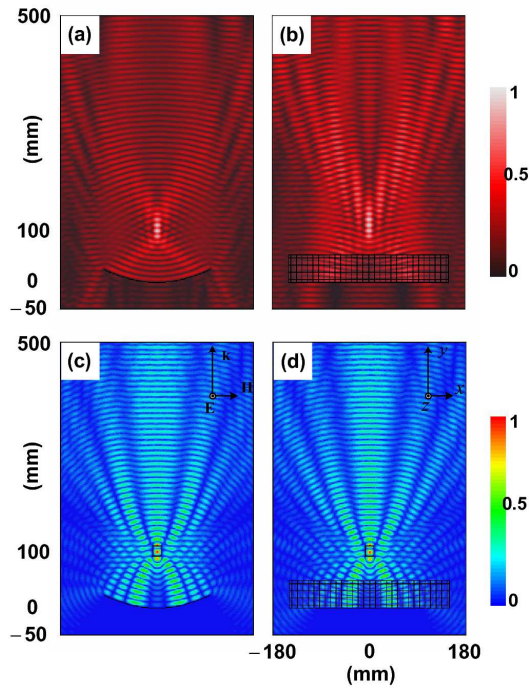

Fig. 2. The normalized E field distribution through the conventional parabolic reflector and 30×5-block flat reflector at 15 GHz. (a) Parabolic reflector and (b) Flat reflector have almost the same convergence at focal point when excited by a plane wave in $\hat{y}$ direction. (c) Parabolic reflector and (d) Flat reflector generate nearly the same plane wave when a waveguide feeding ($0.76\lambda \times 0.34\lambda$) is on the focal points.

Further exploration has been carried out from the practical view concerning the bandwidth as well as the aperture size of the flat reflector [11]. We first replace of the epsilon less than one material by air to remove the dispersive property from those material in the realization. Second, we neglect the material blocks outside the original reflector aperture and keep the transformed reflector from -100 mm to 100 mm which is the same width as the original one. The radiation beams as shown in Fig. 3 between the 20×5-block reflector and the original parabolic one match each other very well. Furthermore, the present compact flat system processes the merits of non-dispersive, isotropic, and lossless material components, where no additional loss such as those from resonating elements in metamaterials is contributed to the structure, which makes it attractive in applications.

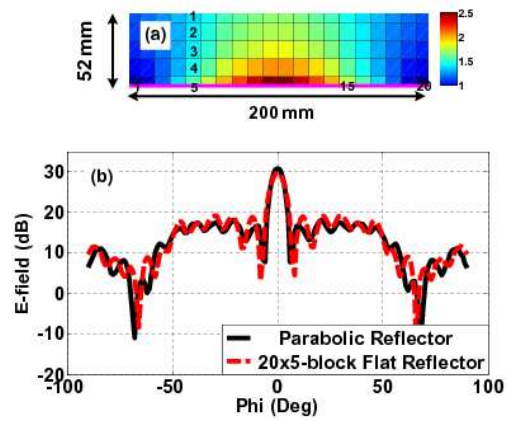

Fig. 3. The Transformed flat reflector and its radiation performance. (a) Flat reflector with the permittivity map consisting of 20×5 dielectric blocks. The five layers have heights of 6.5mm, 13mm, 13mm, 13mm and 6.5mm respectively, and the 1st and 20th unit cells have the width of 6.94mm and the rest from 2nd unit cell to the 19th unit cell have a width of 10.34mm. transformed flat reflector with the permittivity value from 1 to 2.541. (b) The radiation patterns of the parabolic reflector and the 20 × 5-block flat reflector

B. Tunable beam

Achieving highly directive beams from reflectors has been a subject intensively studied and widely adopted to various applications. Meanwhile, a wide angular scanning with such sharp beams is growing a new interest of the explorations [17] which generally involve an operation by simply moving or tilting the feed as shown in Fig. 4(a) and Fig. 4(c). Alternatively, we can achieve the same beam control by moving or tilting the reflector inversely while maintaining the feed on the original focal point as shown in Fig 4(b) and Fig. 4(d). Such schemes utilize the linear/angular displacements within the reflector system to achieve the desired electromagnetic beams, which reveals the essential links between the reflector geometry and the corresponding optical ray-trace.

Transformation optics as a practical strategy provides a straightforward connection between the geometrical optics of lenses and the gradient refractions of electromagnetic materials. Besides the flat profile, the transformed reflector provides another significant advantage that it is composed of 20×5 independent dielectric blocks, which essentially offers another route to manipulate the radiation performance of the reflector. In other words, the reflected emission can be controlled by the permittivity of each dielectric block throughout the aperture. In our case, the linear or the angular

displacement between the feed and reflector thus can be represented by the variation of the permittivity of the dielectric blocks within the transformed reflector.

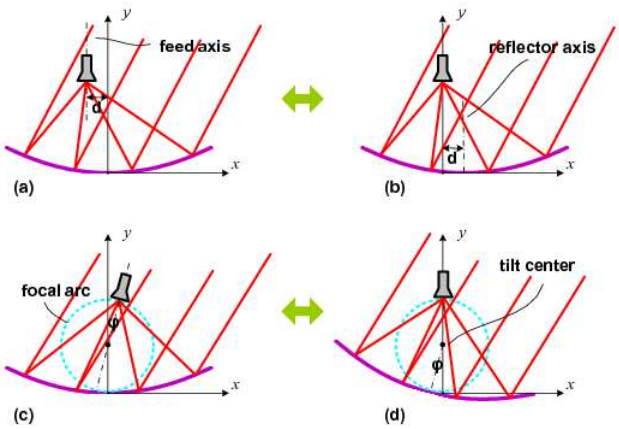

Fig. 4. Scenarios to steer the beam of the parabolic reflector. (a) Moving the feed. (b) Moving the reflector. d refers to the displacement between the feed central axis and the reflector central axis. (a) and (b) have the same effects to control the beam, generally moving feed/reflector will form in a sharp beam on the other/same side of the displacement. (c) Tilting the feed. (d) Tilting the reflector. φ refers to the rotating degree of the feed and reflector around the tilting center. The cyan dashed circle refers to the focal arc when the feed/reflector rotates. (c) and (d) have the same effects to control the beam, generally tilting feed/reflector will form in a sharp beam on the same/other side of the rotating direction.

A full-wave finite-element simulation (Ansoft HFSS v12) is then performed to verify the proposed design. The far field performances of these reflectors are demonstrated in Fig. 3. As is observed, the reflectors have high directivity and the considerably matched radiation patterns as expected at the design frequency of 15 GHz. On the one hand, we can observe that the off-axis feeding will lead to a shift of the main beam for both of the original and transformed reflectors, and approximately every 5 mm displacement will result in 2.5 degree shift for the demonstrate reflector. As a result, 10 mm off-axis feeding as well as the corresponding asymmetric flat reflector in Fig. 2(b) have a 5 degree scanning angle. On the other hand, tilting feed will have the reflector beam redirected, and approximately every 3 degree tilting will lead to 4 degree shifting of the reflected emission, in which 3 degree is from the rotation while another 1 degree is from the off-axis feeding, since the tilting center we chosen here is not the center of the reflector or the feed. As a result, the 9 degree feed tilting as well as the corresponding asymmetric flat reflector in Fig. 2(c) have a 12 degree scanning angle. There is a slight difference between the E-filed patterns, which is because we need to cut and extend the original reflector to do the transformation. However, the overall performance of the transformed flat reflector is considerably nice.

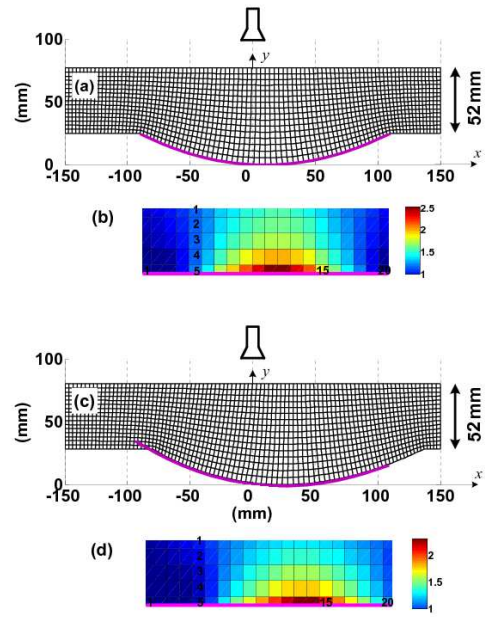

Fig. 5. The quasi-orthogonal mapping of the reflector embeded in the air, and transformed 20×5-block flat reflector. (a) Asymmetric mesh regarding the 10 mm shift of the reflector and the asymmetric transformed flat reflector with the permittivity value from 1 to 2.537. (c) Asymmetric mesh regarding the 9 degree tilting of the reflector and the asymmetric transformed flat reflector with the permittivity value from 1 to 2.317.

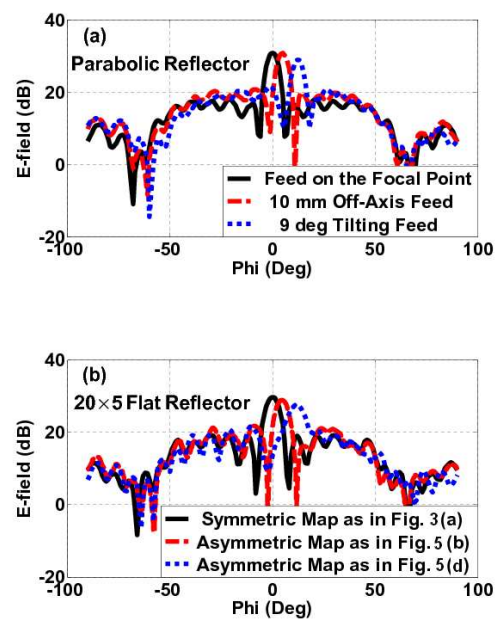

Fig. 6. The radiation patterns of the parabolic reflector and the transformed 20 × 5-block flat reflector. (a) Radiation characteristics of the parabolic reflector with the feed on the focal point, 10 mm off-axis displacement and 9 degree tilting. (b) Radiation characteristics of the corresponding transformed flat reflectors. The main beams of the reflectors for the three scenarios are directed in 0°, 5°, 12° respectively.

III. Conclusion

These investigations validate our design methodology that the reflected emission can be control by only tuning the permittivity values of the dielectric blocks of the flat reflector. In this sense, such a technique will keep no change of flat profile of the reflector system, while processing the ability to steer the radiation beams.

Acknowledgment

Rui Yang's work has been supported by Newton International Fellowship from the Royal Society, U.K.

References

[1] J.B. Pendry, D. Schurig, and D.R. Smith, ``Controlling ElectromagneticFields," Science 312, 1780 (2006).

[2] U. Leonhardt, ``Optical Conformal Mapping," Science 312, 1777 (2006)

[3] D. Schurig, J.B. Pendry, and D.R. Smith, ``Calculation of material properties and ray tracing in transformation media," Opt. Express 14, 9794 (2006).

[4] J. Li and J.B. Pendry, ``Hiding under the carpet: A new strategy for cloaking," Phys. Rev. Lett. 101, 203901 (2008).

[5] R. Liu, C. Ji, J. J. Mock, J. Y. Chin, T. J. Cui, and D. R. Smith, ``Broadband ground-plane cloak," Science, 323, 366 (2009).

[6] J. Valentine, J. Li, T. Zentgraf, G. Bartal, and X. Zhang, ``An optical cloak made of dielectrics," Nature Mater., 8, 568, (2009).

[7] L. H. Gabrielli, J. Cardenas, C. B. Poitras, and M. Lipson, ``Silicon nanostructure cloak operating at optical frequencies," Nature Photon., 3, 461, (2009).

[8] E. Kallos, C. Argyropoulos, and Y. Hao, ``Ground-plane quasicloaking for free space," Phys. Rev. A 79, 063825 (2009).

[9] H.F. Ma, and T.J. Cui, ``Three-dimensional broadband ground-plane cloak made of metamaterials," Nature Communications, 1, 21, (2010).

[10] F. Kong, B.I. Wu, J.A. Kong, J.T. Huangfu, S. Xi, and H.S. Chen, ``Plannar focusing antenna design by using coordinate transformation technology," Appl. Phys. Lett. 91, 253509 (2007).

[11] W. Tang, C. Argyropoulos, E. Kallos, W. Song, and Y. Hao, ``Discrete Coordinate Transformation for Designing All-Dielectric Flat Antennas," IEEE Trans. Antennas Propagat. 58, 3795 (2010).

[12] N. Kundtz and D. R. Smith, ``Extreme-angle broadband metamaterial lens," Nature 9, 129 (2010).

[13] D.A. Roberts, N. Kundtz, and D.R. Smith, ``Optical lens compressionvia transformation optics," Opt. Express 17 16535 (2009).

[14] D.H. Kwon, and D.H. Werner, ``Beam scanning using flat transformation electromagnetic focusing lenses," IEEE Antennas Wireless Propagat. Lett. 8, 1115 (2009).

[15] H.F. Ma, and T.J. Cui, "Three-dimensional broadband and broad-angle transformation-optics lens," Nature Communications, 1, 124, (2010).

[16] R.L. Haupt, ``Adaptive reflector antenna using smart resistive sheets," IET Electron. Lett. 42, 1257 (2006).

[17] S. Silver, ``Microwave Antenna Theory and Design," New York:McGraw-Hill Book Company, (1949).